

Date of publication xxxx 00, 0000, date of current version xxxx 00, 0000.

Digital Object Identifier 10.1109/ACCESS.2017.Doi Number

# A Hierarchical Skull Point Cloud Registration Method

**YANG Wen<sup>1</sup>, ZHOU Mingquan<sup>1,2</sup>, GENG Guohua<sup>1</sup>, LIU Xiaoning<sup>1</sup>**

<sup>1</sup>School of Information Science and Technology, Northwest University, Xi'an 710127, China

<sup>2</sup>School of Information Science and Technology, Beijing Normal University, Beijing 100875, China

Corresponding author: ZHOU Mingquan (e-mail: mqzhou@bnu.edu.cn).

This work was supported by the National Key Research and Development Program of China (2017YFB1402103), National Natural Science Foundation of China (61731015, 61673319, 61802311 and 61902317), Shaanxi Province Industrial Innovation Chain Project of China (2016TZC-G-3-5), Shaanxi Provincial Natural Science Foundation of China (2018JM6061 and 2019JQ-166), Shaanxi Provincial Key Research and Development Program General Project (2019SF-272).

**ABSTRACT** Skull registration is one of the important steps in craniofacial reconstruction, and its registration accuracy and efficiency have an important impact on the reconstruction results. To solve the problem of low accuracy and efficiency of existing skull registration methods, a hierarchical skull point cloud registration method is proposed in this paper. The whole registration process is divided into a rough registration stage and a fine registration stage. Firstly, feature points are extracted from the pre-processed skull point cloud model, and a local coordinate reference system is established according to the feature points and their neighbor points. The improved spin image is used to construct the local feature descriptor. The feature matching is carried out according to the nearest neighbor algorithm, and the k-means algorithm is used to eliminate the mismatching points to achieve skull rough registration. Then, based on rough registration, we use an improved ICP algorithm to achieve fine registration of the skull. In this process, we use random sampling to reduce the search scale of points and add geometric feature constraints to further eliminate mismatched points. Finally, the whole registration algorithm is applied to the skull point cloud data to verify. The experimental results show that, compared with other methods, the registration effect and efficiency of the proposed method are superior to those of other methods. In order to verify the universality of the method, we also use a common data set for verification. Experiments show that the method is also very effective.

**INDEX TERMS** Skull registration, spin image, feature matching, ICP algorithm, random sampling, geometric feature constraints

## I. INTRODUCTION

The identification of the remains of the skull has important applications in the fields of forensic science, anthropology, archaeology, etc. It has always been hot issue research at home and abroad. Craniofacial reconstruction is one of the important ways to identify the skull. There are two main methods for craniofacial reconstruction: traditional manual and computer-aided methods. The manual reconstruction method is greatly influenced by the subjective factors of experts, and the accuracy of the reconstruction results is not high. The computer-aided reconstruction method is the main method currently used. The basic principle of the computer-aided restoration method is to restore the skull  $S$ , find the skull  $S'$  which is most similar to it from the existing skull database, use the face of the skull  $S'$  as the

reference surface of the skull  $S$  to be restored, and then statistically deform the reference surface. Finally, the restoration of the skull to be restored is realized. The process of searching for the most similar skull to the restored skull in the skull database is the skull registration process. It can be seen that the quality of registration results will directly affect the effect of reconstruction. Therefore, it is particularly important to study a high-precision skull registration method.

Skull point cloud registration is an application field of three-dimensional point cloud registration. The task of registration is to solve the conversion relationship between three-dimensional data coordinate points from different perspectives. According to the geometric transformation relationship between three-dimensional point clouds,

registration algorithms are divided into rigid-body transformation-based registration method and non-rigid-body transformation-based registration method. In this paper, only the registration method of rigid body transformation is discussed and studied. For the registration problem of the three-dimensional rigid body model, it is generally divided into two processes: rough registration and fine registration.

Point cloud rough registration can be roughly divided into three categories according to different methods of use: manual registration using tools, point cloud registration based on voting rules and point cloud registration based on local features. Cheng et al. [1] used the label method. Before point cloud registration, labels were added to the model artificially. According to these label feature information, the point cloud information obtained by this method is robust and reliable, but the process is tedious and time-consuming. Aiger et al. [2] proposed a method to extract coplanar a four-point set. The rotation matrix and translation matrix of point cloud data can be quickly calculated by rotation invariant, which has high robustness. Rusu et al. [3] proposed a point feature histogram (FPH) method, which is complex in computation and inefficient in registration. Later, Rusu et al. [4] improved the PFH algorithm and proposed a fast point feature histogram method (FPPH). Compared with the FPH method, this method has higher computational efficiency, but for smaller feature recognition ability is low, and the anti-noise ability needs to be further improved. In addition, there are some registration algorithms using skull region features, normal and curvature features and two-dimensional image features [5-7].

In the fine registration stage, the most classical and widely used algorithm is Iterative Closest Point (ICP) proposed by Besl et al. [8]. ICP algorithm is simple and easy to implement, but it is very time-consuming and easy to fall into local optimum, which may result in incorrect registration results. Therefore, scholars at home and abroad have proposed many improved ICP algorithms. Xie et al. [9] proposed a double interpolation ICP algorithm (FICP), which effectively eliminated outliers and improved the robustness of the ICP algorithm. Choi et al. [10] proposed an improved k-d tree traversal method to speed up the search process of the nearest point, which effectively improved the convergence speed of the algorithm. Bae and Lichti [11] propose an improved ICP algorithm based on point cloud boundary feature points, which effectively improves the efficiency and accuracy of the algorithm. At present, the ICP algorithm is still a hot research method in the registration algorithm [12-13].

Because of complex skull structure, uneven surface, and many holes, it is a very complex three-dimensional point cloud data, so the accuracy of skull registration is required to be higher. Existing registration methods are applied directly to the skull and do not yield the expected

results. Therefore, for the special three-dimensional model of the skull, this paper proposes an improved spin image and ICP method for skull point cloud registration. This method divides the registration process into two parts: rough registration and fine registration. In rough registration, a registration method based on the improved spin image is adopted. Firstly, feature points of the skull point cloud are extracted, the local coordinate system is established according to feature points and their neighboring points, and local feature descriptors based on the improved spin image are calculated. Then, initial corresponding points are searched according to local feature descriptors, and mismatched points are eliminated for rough registration. In fine registration, the registration method based on improved ICP is adopted. In this paper, the ICP algorithm is improved from two aspects of point cloud sampling and mismatched point elimination. The improved algorithm is used in the fine registration process. The process of this method is shown in Figure 1.

This paper is arranged as follows: the first part is the introduction; the second part is skull data acquisition and preprocessing; the third part is skull rough registration; the fourth part is skull fine registration; the fifth part is experimental results and analysis; the last part is the conclusion.

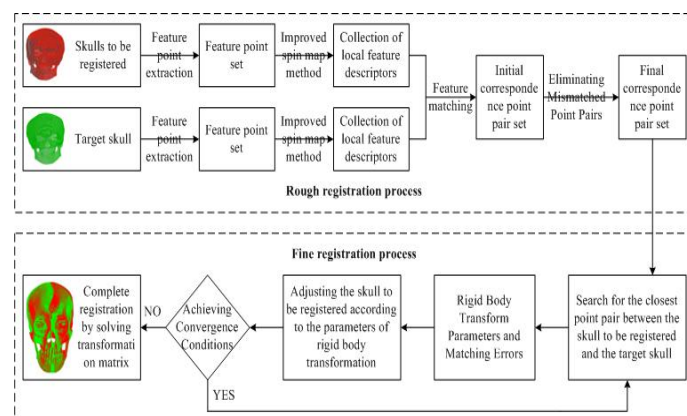


FIGURE 1. Flow chart of the method of this paper

## II. ACQUISITION AND PREPROCESSING OF SKULL DATA

All skull samples in this paper are from the Institute of Visualization Technology, Northwest University. Data acquisition is obtained by using a Siemens multi-detector spiral CT machine and then reconstructed by CT image. The process of skull three-dimensional model reconstruction is realized by the skull reconstruction program independently developed by the research group. All three-dimensional skull models obtained are single-layer 3D point cloud data.

In the CT phase of the skull, the image has been denoised and redundant, but some noise or redundant information can not be completely eliminated by the image processing algorithm. Therefore, after the reconstruction is

completed, the reconstructed three-dimensional model needs to be further processed. After denoising and simplifying the reconstructed model, a clean, small amount of data can be obtained, but the detailed features and geometric shapes of the data can be preserved. In addition, the skull needs coordinate correction and scale normalization. In the coordinate correction, the Frankfurt coordinate system [14] is used to unify the coordinates of all skulls. In scale normalization, the distance from the middle point of the left ear hole to the middle point of the right ear hole, regardless of the size of the skull, is treated as unit 1, that is to say, each vertex of the skull  $(x, y, z)$  is converted to

$$\left( x/|L_p - R_p|, y/|L_p - R_p|, z/|L_p - R_p| \right).$$

Among them,  $L_p$  denotes the middle point of the left ear hole,  $R_p$  denotes the middle point of the right ear hole, and  $L_p - R_p$  denotes the distance from the middle point of the left ear hole to the middle point of the right ear hole.

### III. ROUGH REGISTRATION OF SKULL

The rough registration process is to make the same parts of two three-dimensional models in different coordinate systems that can be roughly matched and coincided. In this paper, the implementation of rough registration is accomplished by using the improved spin image method. Firstly, feature points of the skull point cloud are extracted, and local coordinate system is established according to feature points and their neighboring points, and the local feature descriptors are calculated. Then, according to the local feature descriptor, constraints are applied to find the initial pairs of corresponding points, and the mismatched points are eliminated. Finally, the skull rough registration was performed.

#### A. FEATURE POINT EXTRACTION

The feature point is a set of points on the 3D point cloud that are stable and distinct by defining a particular constraint. Since the number of points on the three-dimensional point cloud is generally large and the processing is complicated, the commonly extracted feature point set together with the local features represents the entire point cloud. The number of feature point sets is much less than the number of 3D point clouds, which can speed up the registration of point clouds, so the selection of feature points is crucial for registration accuracy and speed.

Because the intrinsic shape signature (ISS) method [15] is based on eigenvalue analysis and covariance matrix, the principle of the algorithm is simple and easy to implement. It can process point clouds directly to meet the requirements of skull registration. Therefore, this paper uses the ISS algorithm to extract feature points of the skull point cloud.

For point  $p_i$  on the skull point cloud, the covariance

matrix is calculated by the formula (1) and formula (2). The eigenvalues  $\{\lambda_i^1, \lambda_i^2, \lambda_i^3\}$ ,  $\lambda_i^1 \leq \lambda_i^2 \leq \lambda_i^3$  and the corresponding eigenvectors  $\{e_i^1, e_i^2, e_i^3\}$  are obtained by eigenvalue decomposition of the covariance matrix. A point where the feature value satisfies the condition of the formula (3) is selected as a key point.

$$\bar{p} = \frac{1}{n} \sum_{i=1}^n p_i \quad (1)$$

where  $\bar{p}$  is the centroid of the  $p_i$  neighborhood. Calculate the covariance matrix from  $p_i$  and its neighborhood:

$$C(p_i) = \sum_{N_r(p_i)} (p_i - \bar{p})(p_i - \bar{p})^T \quad (2)$$

where  $N_r(p_i) = \{p_j | \|p_j - p_i\| \leq r\}$  denotes the neighborhood point with  $p_i$  as the center and radius  $r$ .

$$\frac{\lambda_i^2}{\lambda_i^1} < \varepsilon_{12}, \frac{\lambda_i^3}{\lambda_i^2} < \varepsilon_{23} \quad (3)$$

To improve the computational efficiency, we omit the calculation of the local central point. After using the weighted covariance matrix in formula (4), we select the point whose eigenvalue satisfies formula (3) as the key point according to the calculated eigenvalue and add it to the key point set of the skull to complete the extraction of the feature points.

$$C_w = \frac{\sum_{N_r(p_i)} w_j (p_i - p_j)(p_i - p_j)^T}{\sum_{N_r(p_i)} w_j}, \quad (4)$$

$$w_j = \frac{1}{\|p_j - p_i\|}, \forall p_j \in N_r(p_i)$$

For each point  $p_j$  in the neighborhood of the key point, the weight  $w_j$  is inversely proportional to the Euclidean distance between point  $p_j$  and  $p_i$ . The weight is used to improve the robustness of LRF to occlusion, clutter, and local resolution changes.

#### B. ESTABLISHMENT OF LOCAL COORDINATE SYSTEM

The local coordinate reference system is established based on the key points and their neighbor points. It does not change with the change of the measurement viewpoint. When extracting the local features, the local coordinate reference axis is established according to the data of the key support domain, and The local coordinate descriptor is extracted in the local coordinate system. The local coordinate reference system can provide an effective reference for the extraction of local features such that the local features have rotational and translation invariance.

To construct the local coordinate reference system at the key point, firstly, the sphere with the radius  $r$  is

centered on the key point, and the local neighbor point of the point is obtained from the point cloud. Let the set of key points of skull be  $\mathbf{P}_K = \{p_i\}_{i=1}^{N_K}$ ,  $N_K$  is the number of key points, and the eigenvectors of each key point are  $\{e_i^1, e_i^2, e_i^3\}$ . Therefore, LRF can determine  $z$  axis by formula (5).

$$z(p_i) = \begin{cases} e_i^1, & e_i^1 \cdot \sum_{j=1}^{n_r} p_i p_j \geq 0 \\ -e_i^1, & \text{otherwise} \end{cases} \quad (5)$$

where  $p_i p_j = p_j - p_i$  represents the vector from point  $p_i$  to point  $p_j$ .

The  $x$ -axis and the  $y$ -axis are determined by the method of Yang et al. [16], and the tangent plane at the  $p_i$  point can be constructed from the normal vector  $n_i = z(p_i)$  of the  $p_i$  point and the point  $p_i$ . The point in  $N_r(p_i)$  is projected to the tangent plane, and the projection vector  $v_{ij}$  of each neighborhood  $p_j$  point in the tangent plane is calculated.

$$v_{ij} = (p_i p_j) - (p_i p_j \cdot z(p_i)) \cdot z(p_i) \quad (6)$$

The weighted average of all projection vectors  $v_{ij}$  of tangent plane at  $p_i$  is used to estimate the  $x$ -axis.

$$x(p_i) = \frac{\sum_{j=1}^{n_r} w_{j1} w_{j2} v_{ij}}{\left\| \sum_{j=1}^{n_r} w_{j1} w_{j2} v_{ij} \right\|} \quad (7)$$

where  $w_{j1} = (r - \|p_j - p_i\|)^2$  denotes the weight of the distance between  $p_j$  and  $p_i$ , and  $w_{j2} = ((p_j - p_i) \cdot n_i)^2$  denotes the projection weight between them.  $\|\cdot\|$  denotes the  $L_2$  norm. The first weight  $w_{j1}$  is to improve the robustness of the local coordinate system to clutter and occlusion. Therefore, the distant neighborhood points contribute less to the  $x$ -axis. The second weight  $w_{j2}$  is to make the point with larger projection distance contribute more to the  $x$ -axis, and can provide higher repeatability in the plane area.

Finally, the  $y$ -axis of LRF is determined by the following way, and its direction is determined according to the right hand rule.

$$y(p_i) = z(p_i) \times x(p_i) \quad (8)$$

Therefore, the local reference coordinate system at the feature point  $p_i$  can be established by the above algorithm.

$$L(p_i) = \{x(p_i), y(p_i), z(p_i)\} \quad (9)$$

### C. LOCAL FEATURE DESCRIPTOR BASED ON IMPROVED SPIN IMAGE

Spin image [17] is a method of representing local feature descriptors with grid images. It has translation and rotation invariance. The spin image has a relatively stable effect on rigid-body transformation. It has been widely used in point cloud registration. But there are still some problems: (1) Because spin image is the statistics of neighborhood points of key points, they are affected by the density of neighborhood points and noise points. (2) Spin image is obtained by transforming data from three-dimensional space to two-dimensional space, abandoning angle information and using only local surface normal vectors as reference axes, which contain less information. (3) The matching process of the spin image is time-consuming. In this paper, the spin image is improved based on the problems of the spin image and the inspiration of the Trisi local features proposed by Guo et al. [18].

The improvement lies in: The original method is: when all the points in the  $P$  neighborhood are represented by spin coordinates  $(\alpha, \beta)$ , the two-dimensional space is divided into  $L \times L$  grids, and the number of points in each grid is accumulated, which can be obtained. A two-dimensional digital image, which is a spin image. The improved method is as follows: when all points in  $P$  neighborhood are represented by spin coordinates  $(\alpha, \beta)$ , the two-dimensional space is divided into  $L \times L$  grids, and the number of neighborhood points falling into each lattice is counted, thus  $L \times L$  number distribution matrices are obtained, and the average number distribution matrix is used to describe local features. To reduce the feature dimension, the information of the average distribution matrix is extracted and compressed to obtain a robust local feature descriptor.

Let  $P$  be the key point of the skull key point set and the local coordinate reference system of  $P$  is  $L(p) = \{x(p), y(p), z(p)\}$ . With the  $P$  point as the center, the neighborhood point with radius  $r_s$  is  $N_{r_s}(p) = \{p_j \mid \|p_j - p\| \leq r_s\}$ . The steps of local feature calculation are as follows:

**Step1:** A cylindrical coordinate system is constructed with  $P$  as the origin and the coordinate axis  $x(p)$  of the point as the main direction, and the neighboring points of the point are substituted into the formula (10) to obtain the spin coordinates  $(\alpha_j, \beta_j)$  of the neighboring point  $p_j$  of the key point  $P$ . Let  $\lambda$  be the largest absolute value of  $\alpha$  and  $\beta$  in the spin coordinates of neighboring points, let

$\alpha_j = \frac{a_j}{\lambda}$ ,  $\beta_j = \frac{\beta_j}{\lambda}$ , and then the normalized spin coordinates are  $(\alpha_j, \beta_j)$ .



$$\alpha = \sqrt{\|q - p\|^2 - (n \cdot (q - p))^2}$$

$$\beta = n \cdot (q - p)$$
(10)

**Step2:** All the normalized spin coordinates obtained in the previous step are divided into  $L \times L$  coordinate grids in two-dimensional space, and each spin coordinate is recorded in the grid. The number of neighborhood points in each grid is counted, and then  $L \times L$  number distribution matrices are obtained, which is recorded as  $\mathbf{D}^1$ .  $\mathbf{D}^1$  reflects the distribution of neighborhood points in two-dimensional space. We use the average quantity distribution matrix to describe the local features. The calculation method is as follows:

$$\overline{\mathbf{D}^1} = \frac{\mathbf{D}^1}{|N_{r_s}(p)|}$$
(11)

**Step3:** In order to reduce the dimension of the feature, the information of the average number distribution matrix is further extracted and compressed. Because the low-order center moments  $u_{11}, u_{12}, u_{21}, u_{22}$  and Shannon entropy  $e$  contain most useful information of average distribution matrix  $\overline{\mathbf{D}^1}$ , and the low-order center distance is more robust to noise and resolution changes, this paper uses the center moments and Shannon entropy to extract information in the matrix, that is,  $F^1 = \{u_{11}, u_{12}, u_{21}, u_{22}, e\}$ , in which the  $m+n$  order center moments of average distribution matrix  $\overline{\mathbf{D}^1}$  are defined as:

$$u_{mn} = \sum_{i=1}^L \sum_{j=1}^L (i - \bar{i})^m (j - \bar{j})^n \overline{\mathbf{D}^1}(i, j),$$

$$\bar{i} = \sum_{i=1}^L \sum_{j=1}^L i \overline{\mathbf{D}^1}(i, j), \bar{j} = \sum_{i=1}^L \sum_{j=1}^L j \overline{\mathbf{D}^1}(i, j)$$
(12)

**Step4:** After the description vector  $F^1$  is obtained, the point  $P$  is taken as the origin again, and the  $y(p)$  and  $z(p)$  of the point coordinate axis are used as the main direction to form the cylindrical coordinate system of the point, and the other two description vectors  $F^2$  and  $F^3$  are calculated. By concatenating the three descriptor vectors in series, a more discriminative descriptor vector  $F = \{F^1, F^2, F^3\}$  is obtained. Finally, the key point  $P$ , its local coordinate reference system  $L(p)$  and its local descriptor  $F$  form a robust local feature descriptor  $f = \{p, L(p), F\}$ .

#### D. ROUGH REGISTRATION PROCESS

After obtaining the local feature descriptors, the corresponding points with the smallest distance between the feature descriptors are selected as the initial corresponding points for feature matching. The purpose of feature

matching is to establish the corresponding relationship between feature points, but there will be mismatching point pairs in the matching process. After eliminating the mismatching point pairs, the skull coarse registration will be realized finally.

To improve the accuracy of rough registration, the nearest neighbor algorithm combined with a threshold is used to further improve the accuracy of feature matching. The matching process is as follows:

**Step1:** The source point cloud  $P_S$  and the target point cloud  $P_T$  are assumed to extract the key points, and the corresponding key point sets  $P_i$  and  $P_j$  are obtained. Then the local features  $M_i = \{f_1^i, f_2^i, \dots, f_{N_i}^i\}$  and  $M_j = \{f_1^j, f_2^j, \dots, f_{N_j}^j\}$  of the point set  $P_i$  and  $P_j$  are calculated, where  $N_i$  and  $N_j$  represent the size of  $P_i$  and  $P_j$  respectively.

**Step2:** For each feature  $f_k^i$  in  $M_i$ , its nearest feature  $f_k^j$  in  $M_j$  is calculated. When the formula (13) is satisfied and the closest distance between them is less than the threshold  $\delta_d$ , it is considered that  $f_k^i$  and  $f_k^j$  constitute a corresponding point pair, expressed as  $c_k^{ij} = \{f_k^i, f_k^j\}$ , all corresponding point sets generate  $\mathbf{C}^{ij}$ .

$$F_k^j = \arg \min_{n=1,2,\dots,N_{Q_k}} (\|F_k^i - F_k^j\|)$$
(13)

There is a mismatching point in the initial corresponding point set obtained by the feature matching, which results in a large error in the transformation relationship obtained by the initial corresponding point set. Therefore, it is necessary to adopt appropriate methods to remove mismatched points from the initial set of corresponding points, to make the transformation relationship between skulls more accurate. In this paper, we use the k-means algorithm to eliminate mismatch pairs.

For each corresponding point pair  $c_k^{ij}$ , using its coordinates  $(p_k^i, p_k^j)$  and local coordinate reference systems  $(L(p_k^i), L(p_k^j))$ , the rotation matrix  $R_k^{ij}$  and translation vector  $t_k^{ij}$  are calculated by the following formulas, forming a rigid transformation relationship  $T_k^{ij} = \{R_k^{ij}, t_k^{ij}\}$ .

$$R_k^{ij} = L(p_k^j)(L(p_k^i))^T$$
(14)

$$t_k^{ij} = p_k^i - R_k^{ij} p_k^j$$
(15)

There are  $N_{ij}$  key point pairs in  $\mathbf{C}^{ij}$ , so the rigidity of

$N_{ij}$  can be obtained according to the above formula. A new set  $TF$  is formed by transforming the rotation matrix of  $N_{ij}$  into a seven-dimensional vector composed of quaternions and translation vectors. Then, the k-means algorithm is used to cluster the new set. At the end of the clustering, the point pair set  $C_k^{ij}$  of the least error class is retained as the final result.

#### IV. FINE REGISTRATION OF SKULL

The method in Section 3 of this paper has coarsely registered the skull point cloud and obtained the relationship between the initial registration point pair and the feature matching. However, due to the huge amount of point cloud data, the registration is caused by mismatched points in the initial registration process. The accuracy is not high. Therefore, on the basis of rough registration, further fine registration of the point cloud is needed. In the fine registration process of the skull, we use a modified ICP algorithm to achieve registration. However, the ICP algorithm is directly applied to the registration of skull point clouds, and the effect is not satisfactory. Therefore, there is a need to improve the ICP algorithm. This paper improves from the sampling of the point cloud and the elimination of mismatched points.

Each iteration of the standard ICP algorithm searches all points on the point cloud for the closest point on the target point cloud. However, due to a large number of point clouds, the algorithm is time-consuming, and every iteration, all points of point clouds are registered, so the registration error is large. Therefore, this paper uses a part of the point set to speed up the search of corresponding point pairs and accelerate the iteration process.

For source point cloud  $P_S$  and target point cloud  $P_T$ , we use a random sampling method to select a part of the total point set randomly for searching the nearest point in each iteration. At the  $k$ th iteration,  $n_k$  points on the point cloud  $P_S$  are randomly used to search for their closest point on  $P_T$ . Where  $n_p$  is the total number of source point clouds,  $d_{avg}$  is the average distance between points,  $\omega$  is the parameter of control points,  $\ell_{k-1}$  is the error of an iteration.

$$n_k = -\frac{1}{4} \ln \left( \frac{\ell_{k-1}}{d_{avg}} \right) \omega n_p \quad (16)$$

From the above formula, we can see that the number of points selected for each iteration is related to the error. In the early stage of iteration, registration error is large, so the number of points selected is small. As the number of iterations increases and registration error decreases, we can increase the number of sampling points to achieve more fine registration.

After rough registration, the source point cloud and the target point cloud are basically located in the same coordinate system, and the geometric characteristics of the point pairs are similar in their neighborhoods. Therefore, in the process of searching for corresponding points, by adding geometric feature constraints, the pairs of mismatched points can be eliminated, the corresponding pair of points can be quickly determined, and the efficiency of searching can be improved. In this paper, the constraint of the corresponding point pair is performed by calculating the distance between the two nearest point pairs  $p^i$  and  $q^j$  and the coordinate origin  $O$ , and the angle  $\phi_n$  between the two matching point normal vectors. The distance between  $p^i$  and the origin of coordinates is  $d^i$ , the distance between  $q^j$  and the origin of coordinates is  $d^j$ , and their normal vectors are  $n^i$  and  $n^j$ , respectively, and the angle between them is  $\phi$ . Therefore, the mismatching points can be eliminated by the following constraints:

$$\|d^i - d^j\| \leq \varepsilon_d \cap \sin \phi_n \leq \varepsilon_\phi \quad (17)$$

Through the above constraints, the corresponding pairs that do not satisfy the condition can be excluded, and the corresponding pairs that satisfy the condition can be added to the set of corresponding pairs.

#### V. ANALYSIS OF EXPERIMENTAL RESULTS

This algorithm is implemented in Intel Core i7 3.41 GHz CPU, 8G memory PC, Visual studio 2015 software using C++ language and PCL point cloud library. The 90 sets of skull point cloud data used in the experiment were all reconstructed by CT scanning. In the experiment, we defined the quantitative evaluation index of the accuracy of the registration results, validated the skull rough registration method and the skull fine registration method proposed in this paper, and validated the universality of the algorithm by using common data sets.

##### A. QUANTITATIVE EVALUATION OF ACCURACY OF REGISTRATION RESULTS

Because of the similarity between skulls, in order to evaluate the accuracy of skull point cloud registration more directly, we use root mean square error (RMSE) to quantify the results of skull registration and measure the accuracy of skull registration.

$$RMSE = \sqrt{\frac{1}{N_p} \sum_{i=1}^{N_p} \|Rp_i + T - q_j\|} \quad (18)$$

where  $N_p$  represents the matching point logarithm and  $q_j$  is the point in the point set  $Q$  that matches  $p_i$ .

##### B. EXPERIMENTAL RESULTS AND ANALYSIS OF SKULL ROUGH REGISTRATION

In the rough registration of the skull, we used 90 sets of skull point cloud data as the test sample for rough

registration and calculated the root mean square error to evaluate the registration results. To verify that the proposed method has better accuracy and higher efficiency, the method is compared with the PCA-based rough registration algorithm [19] and the curvature-based rough registration algorithm [20]. In the experiment, there were 207487 points in the skull to be registered and 210304 points in the target skull. The number of key points extracted was 695 and 698, respectively. The results of registration between the skull to be registered and the target skull are shown in Fig. 2. The efficiency comparison of rough registration is shown in Table 1.

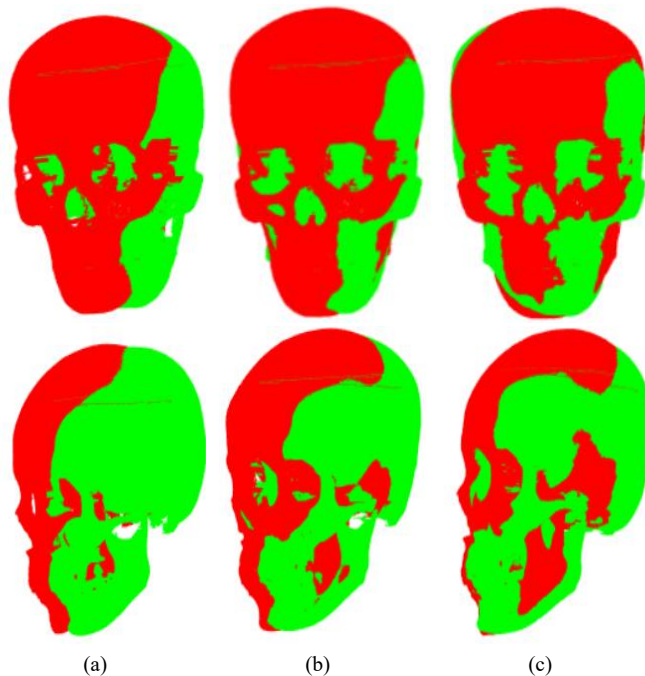


**FIGURE 2.** Comparison of skull rough registration results. (a) Rough registration based on PCA, (b) Rough registration based on curvature graph, and (c) The method in this paper.

**TABLE 1.** Comparison of Rough Registration Efficiency

Algorithm		Rough registration based on PCA	Rough registration based on curvature graph	The method in this paper
Registration of the skull to be registered with the target skull	Registration error (mm)	$8.031 \times 10^{-1}$	$6.233 \times 10^{-1}$	$4.658 \times 10^{-1}$
	Time-consuming algorithm (s)	23.38	30.24	16.11

As can be seen from Figure 2, the registration effect of this paper is the best. Taking the mandibular part of the skull as an example, after registration based on PCA method and curvature map method, the mandibular part of the two skulls does not completely coincide, but the two skulls coincide well after registration by this method, which shows that the positions of the two skulls are basically the

same. The registration errors of the three methods and the running time of the algorithm are calculated for two groups of experiments, respectively, as shown in Table 1. Compared with PCA-based rough registration method and curvature-based rough registration algorithm, the registration error of this paper is the smallest, and the algorithm is also the least time-consuming.

Therefore, compared with the other two algorithms, the proposed algorithm effectively reduces the time complexity of rough registration and improves the accuracy of registration. Through rough registration, it can be seen that the two skulls are almost in the same coordinate system.

### C. EXPERIMENTAL RESULTS AND ANALYSIS OF SKULL FINE REGISTRATION

In the fine registration of the skull, the selected 90 sets of skull data were used as samples, and the standard ICP algorithm and the improved ICP algorithm were used for registration, and the results and efficiency of the registration were compared and analyzed.

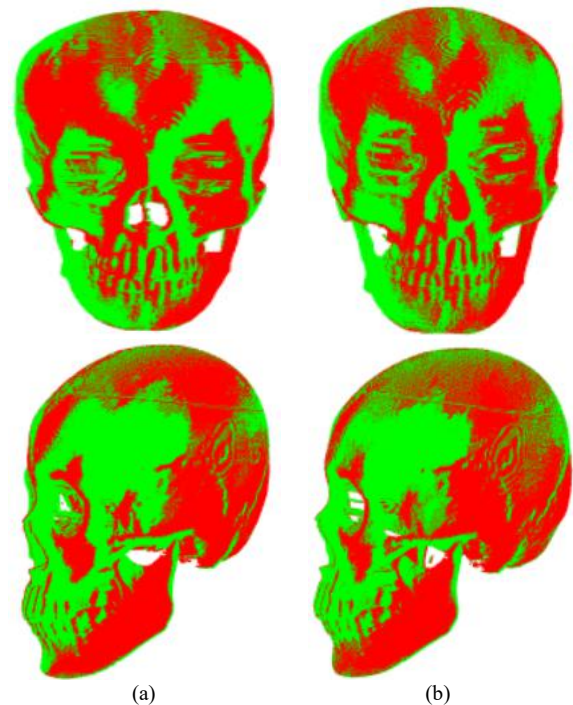


**FIGURE 3.** Comparison of Skull Fine Registration Results. (a) Standard ICP algorithm, and (b) Improved ICP algorithm.

**TABLE 2.** Comparison of Fine Registration Efficiency

Algorithm	Number of iterations	Registration error (mm)	Time-consuming algorithm (s)
Standard ICP algorithm	56	$7.843 \times 10^{-2}$	67.164
Improved ICP algorithm	32	$6.108 \times 10^{-2}$	31.322

From the results of fine registration in Figure 3, we can see that both algorithms can achieve better results, and it may be difficult to distinguish which method works better visually. However, from the experimental data in Table 2, it



can be seen that the standard ICP algorithm needs 56 iterations to achieve fine registration of the skull, while this algorithm only needs 32 iterations to achieve fine registration. Because this method improves the sampling point selection and culling mismatch points of the ICP algorithm, the matching speed is accelerated, and the number of iterations required is also reduced. Therefore, the proposed method is less time-consuming and more accurate for fine registration.

#### D. EXPERIMENT RESULTS AND ANALYSIS OF ROUGH REGISTRATION + FINE REGISTRATION

To verify the effectiveness of the whole algorithm, the skull samples are roughly registered and then accurately registered. Comparing the proposed algorithm with curvature-based rough registration algorithm + standard ICP algorithm (curvature + ICP) and PCA-based rough registration algorithm + standard ICP algorithm (PCA + ICP), the efficiency of the proposed algorithm is verified.

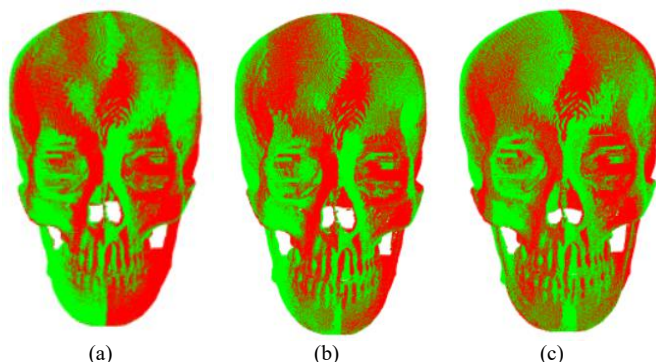


FIGURE 4. Comparison of registration results of different registration algorithms. (a)PCA + ICP, (b)Curvature + ICP, and (c)The algorithm in this paper.

TABLE 3. Comparison of different registration algorithms efficiency

Algorithm	Number of iterations	Registration error (mm)	Time-consuming algorithm (s)
PCA + ICP	37	$4.973 \times 10^{-2}$	61.321
Curvature + ICP	31	$3.247 \times 10^{-2}$	64.186
The method in this paper	24	$1.962 \times 10^{-2}$	36.089

From Figure 4, we can see that the three registration algorithms have achieved relatively high accuracy. Through comparative observation, the algorithm in this paper is more uniform in the skull and mandible registration, and the registration effect is better. Through the analysis of Table 3, compared with the other two algorithms, the registration accuracy and time-consuming of the proposed algorithm are significantly improved. Due to a large number of skull point clouds, if the nearest point is searched for all points, the time consumption is obviously increased; and there are many mismatches in the matching process, and there may be a large difference between the initial positions of the two skulls. These will affect the registration results and efficiency. Therefore, in the coarse registration stage, we adjust the initial positions of two skulls, to improve the sampling points and mismatching

points in the fine registration stage, to reduce the number of iterations, improve the accuracy of registration and reduce the time-consuming.

#### E. VERIFICATION OF ALGORITHMIC UNIVERSALITY

Based on the above experimental results and analysis, this method has achieved a good registration effect on the skull data. To further verify the effectiveness of the proposed method, we validate the method using a common data set. The experimental data were validated by the rabbit model of Stanford University in the rough registration stage, the precise registration stage and the complete process of rough registration + fine registration.

##### 1) UNIVERSALITY VERIFICATION OF ROUGH REGISTRATION ALGORITHMS

In the rough registration experiment, the rabbit point cloud model is used as the object, and the rough registration method based on spin image, the rough registration method based on FPFH and the improved spin image proposed in this paper are used for registration. The registration errors and algorithm time-consuming of each method are calculated, and the registration results and efficiency are analyzed. There are 40256 points in the point cloud model of the rabbit to be registered and 40097 points in the target rabbit point cloud model. The key points extracted are 131 and 120, respectively. The rough registration results of the rabbit model are compared as shown in Figure 5. The registration efficiency pairs are shown in Table 4.

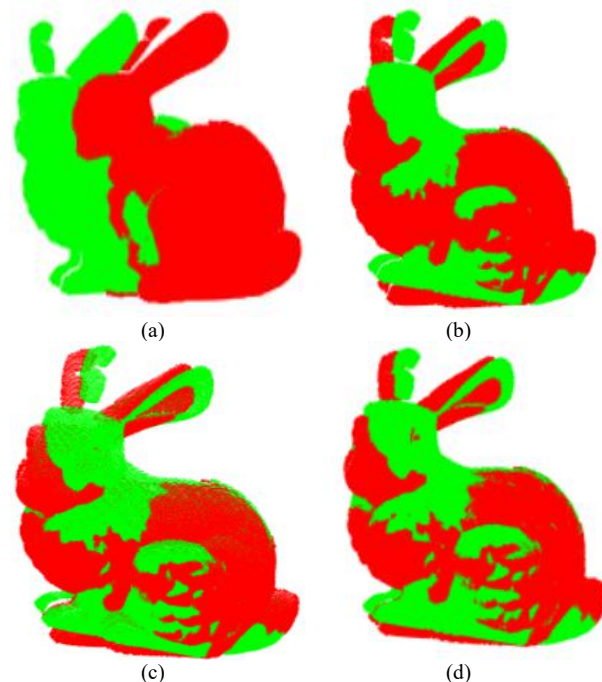


FIGURE 5. Comparison of rough registration results of rabbit models. (a)initial position, (b)Rough registration method based on spin image, (c)Rough registration method based on FPFH, and (d)The method in this paper.

TABLE 4. Comparison of Rough Registration Efficiency of Rabbit Model



Algorithm		Rough registration method based on spin image	Rough registration method based on FPFH	The method in this paper
Bunny Model	Registration error (mm)	$8.317 \times 10^{-2}$	$6.429 \times 10^{-2}$	$4.753 \times 10^{-2}$
	Time-consuming algorithm (s)	2.49	2.64	3.21

The two contrastive algorithms are similar in process to the algorithm in this paper, which is of great reference significance. The experimental results show that, compared with the other two algorithms, the time-consuming of the proposed algorithm is increased, but the registration accuracy is improved obviously. Compared with the spin image method, since the method contains more information on the direction, the registration accuracy is more obvious than the spin image. Compared with the FPFH method, the proposed algorithm has stronger anti-noise ability, so the registration accuracy is better.

## 2) UNIVERSALITY VERIFICATION OF FINE REGISTRATION ALGORITHMS

In the fine registration experiment, the rabbit point cloud model is taken as the object, and the standard ICP algorithm and the improved ICP algorithm are used for registration. The registration errors and algorithm time-consuming of the two methods are calculated, and the registration results and efficiency are analyzed.

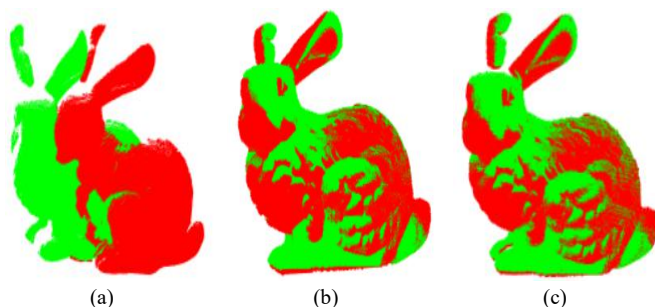


**FIGURE 6.** Comparison of fine registration results of rabbit models. (a)Initial position before registration, (b)Standard ICP algorithm, and (c)Improved ICP algorithm.

**TABLE 5.** Comparison of Fine Registration Efficiency of Rabbit Model

Algorithm		Number of iterations	Registration error (mm)	Time-consuming algorithm (s)
Bunny Model	Standard ICP algorithm	38	$9.369 \times 10^{-3}$	22.672
	Improved ICP algorithm	26	$7.108 \times 10^{-3}$	13.284

Figure 6 (a) is the initial position of the two point clouds, and there is little difference between them. It can be seen from Figure 6 (b) and Figure 6 (c) that the registration effect of the two methods is better. However, it can be seen from the foot, ears and bottom of the rabbit point cloud data that the improved ICP algorithm has higher precision than

the standard ICP algorithm.

It can be seen from Table 5 that, based on the same experimental data, compared with the standard ICP algorithm, the improved ICP algorithm proposed in this paper is significantly improved in both registration accuracy and algorithm time consumption. The standard ICP algorithm is iterative 38 times to achieve registration, the registration accuracy is  $9.369 \times 10^{-3}$ mm, and the algorithm time is 22.672s. The algorithm in this paper is superior to the standard ICP algorithm in iterations, registration accuracy and time-consuming. This is because the algorithm in this paper searches for the corresponding points, and eliminates the mismatched pairs by adding geometric feature constraints to quickly and accurately determine the corresponding pair of points, which improves the search efficiency.

## 3) UNIVERSAL VERIFICATION OF ROUGH REGISTRATION AND FINE REGISTRATION

Therefore, this paper takes the rabbit point cloud data with initial position at 0 degree and 90 degrees as the experimental object, respectively adopts the spin image based coarse registration algorithm + standard ICP algorithm (SI + ICP), FPFH based registration algorithm + standard ICP algorithm (FPFH + ICP) and this paper The proposed rough registration algorithm + fine registration algorithm are combined to carry out comparative experiments to verify the effectiveness of the proposed algorithm.

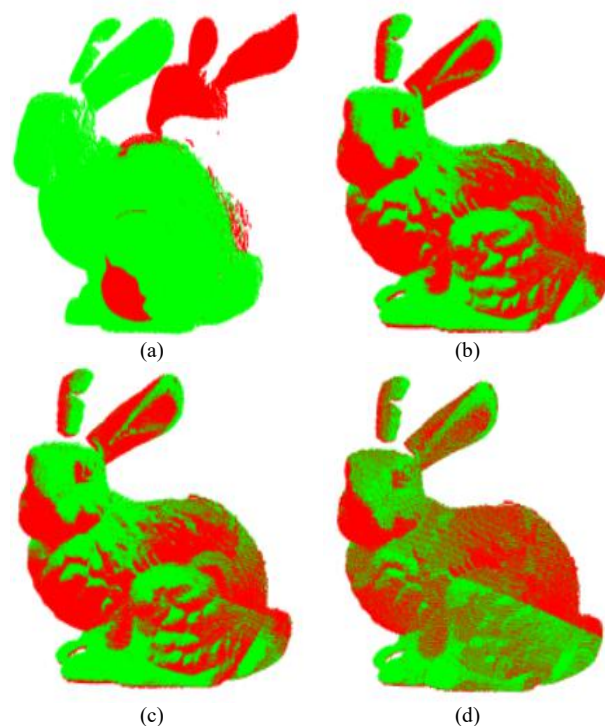


**FIGURE 7.** Comparison of Rough Registration and Fine Registration of Rabbit Model. (a)Initial position before registration, (b)SI+Standard ICP algorithm, (c)FPFH+Standard ICP algorithm, and (d)The method in this paper.

**TABLE 6.** Comparison of Rough Registration and Fine Registration Efficiency of Rabbit Model

Algorithm	Number of iterations	Registration error (mm)	Time-consuming algorithm (s)
SI + Standard ICP algorithm	33	$5.353 \times 10^{-3}$	26.167
FPFH + Standard ICP algorithm	29	$4.289 \times 10^{-3}$	24.083
The method in this paper	22	$2.195 \times 10^{-3}$	15.651

From the registration effect of Figure 7, we can see that the algorithm in this paper is better than the other two methods. From the rabbit's ear, back and other positions, we can see that the registration results of the algorithm in these parts are more uniform and basically coincide. From the quantitative point of view, it can be seen from Table 6 that compared with the other two methods, the algorithm in this paper has the least number of iterations and achieves a better registration effect when iterating 22 times. Moreover, the registration accuracy and time-consuming of this algorithm are better than the other two methods. Compared with SI + standard ICP, this paper also uses SI + ICP combination, but this paper improves SI in rough registration. The characteristics of SI contain less information and are affected by the density of neighborhood points. The improved SI is optimized for these issues, so results and efficiency are better. Compared with the FPFH + standard ICP, this paper mainly improves the standard ICP algorithm. We reduce the search scale by random sampling, which shortens the time consumption. Geometric constraints are used to eliminate mismatched pairs, and then registration is more accurate.

## VI. CONCLUSION

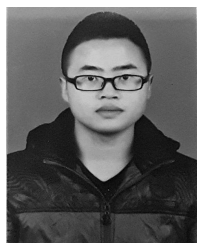
This paper presents an improved skull registration method based on spin image and ICP. Firstly, the skull model is denoised and normalized, the key points of the skull point cloud are extracted, and the local coordinate reference system is constructed according to the key points and their neighbor points. Subsequently, local feature descriptors are constructed based on the improved spin image to constrain and find the initial corresponding point pairs to achieve skull rough registration, which provides a good initial condition for fine registration. Then, on the basis of rough registration, the improved ICP algorithm is used to achieve accurate registration. Finally, the whole registration algorithm is applied to the skull point cloud data. The experimental results show that, compared with other registration methods, the accuracy and efficiency of this method are significantly improved, and it is also effective in public data sets. The contribution of this method is as follows: 1, In the rough registration stage, the method of the spin image is improved. The average number distribution matrix is used to describe local features, which overcomes the influence of neighborhood point density and enriches the information contained in local descriptors. The

method of combining the nearest neighbor algorithm with a threshold is used to improve the accuracy of feature matching, and the k-means algorithm is used to eliminate mismatching points. 2, In the fine registration stage, the standard ICP algorithm is improved, random sampling is used to narrow the search scale, and the search speed is improved. The geometric feature constraints are added, the mismatched pairs are eliminated, the corresponding point pair sets are quickly determined, and the precision is improved.

## REFERENCES

- [1] Cheng L, Tong L, Li M, et al. Semi-Automatic Registration of Airborne and Terrestrial Laser Scanning Data Using Building Corner Matching with Boundaries as Reliability Check[J]. Remote Sensing, 2013, 5(12): 6260–6283
- [2] Aiger D, Mitra N J, Cohen-Or D. 4-points congruent sets for robust pairwise surface registration[J]. ACM Transactions on Graphics, 2008, 27(3): 1-11
- [3] Rusu R B, Blodow N, Beetz M. Persistent point point feature histograms for 3D point clouds [C]. IEEE/RSJ International Conference on Intelligent Robots and Systems, 2008:3384-3391
- [4] Rusu R B, Blodow N, Beetz M. Fast point feature histograms for 3D registration [C]. IEEE International Conference on Robotics and Automation, 2009: 3212-3217
- [5] CAO Z C, MA F L, FU Y L, et al. A Scale Invariant Interest Point Detector in Gabor Based Energy Space[J]. Acta Automatica Sinica, 2014, 40(10): 2356-2363
- [6] IZUMIYA S, NABARRO A C, SACRAMENTO A D J. Pseudo-spherical Normal Darboux Images of Curves on a Timelike Surface in Three Dimensional Lorentz Minkowski Space[J]. Journal of Geometry and Physics, 2015, 97: 105-118
- [7] LIN C C, TAI Y C, LEE J J, et al. A Novel Point Cloud Registration Using 2D Image Features[J]. Eurasip Journal on Advances in Signal Processing, 2017(1): 5-15
- [8] Besl P J, McKay N D. A method for registration of 3D shapes[J]. IEEE Transactions on Pattern Analysis and Machine Intelligence, 1992, 14(2): 239-256
- [9] Xie Z, Xu S, Li X. A high-accuracy method for fine registration of overlapping point clouds[J]. Image and Vision Computing, 2010, 28(4): 563-570
- [10] Choi W S, Kim Y S, Oh S Y, et al. Fast iterative closest point framework for 3D LIDAR data in intelligent vehicle[C]. //Proceedings of the IEEE Intelligent Vehicles Symposium. Spain: Madrid, 2012: 1029-1034
- [11] Bae K and Lichti D D. A method for automated registration of unorganised point clouds[J]. ISPRS Journal of Photogrammetry and Remote Sensing, 2008, 63(1): 36–54
- [12] Ge Y Q, Wang B Y, Nie J H, et al. A point cloud registration method combining enhanced particle swarm optimization and iterative closest point method [C]. //Chinese Control and Decision Conference, Yinchuan: IEEE, 2016. doi: 10.1109/CCDC.2016.7531460
- [13] Li W M, Song P F. A modified ICP algorithm based on dynamic adjustment factor for registration of point cloud and CAD model[J]. Pattern Recognition Letters, 2015, 65: 88-94
- [14] Yang W, Liu X N, Zhu F, et al. Determination of Sex Discriminant Function Analysis in Chinese Human Skulls[C]. Biometric Recognition. CCB 2018. Lecture Notes in Computer Science, vol 10996. Springer, Cham
- [15] Zhong Y. Intrinsic shape signatures: A shape descriptor for 3D object recognition[C]. //Computer Vision Workshops (ICCV Workshops), 2009 IEEE 12th International Conference on. IEEE, 2009
- [16] Yang J Q, Zhang Q, Xiao Y, et al. TOLDI: An effective and robust approach 3D local shape description [J]. Pattern Recognition, 2017, 65: 175-187

- [17] Johnson A E, Hebert M. Surface matching for object recognition in complex three-dimensional scenes[J]. Image and Vision Computing, 1998, 16(9-10): 635-651
- [18] Guo Y, Sohel F, Bennamoun M, et al. Trisi: A distinctive local surface descriptor for 3d modeling and object recognition. The 8th International Conference on Computer Graphics Theory and Applications, 2013, pp.86-93
- [19] Wang YJ, Wu MM, Gao Q. 3D point cloud registration algorithm based on locality preserving PCA[J]. Optical Technology, 2018, 44:562-568
- [20] Ge BZ, Peng B, Tian QG. Registration of Three-Dimensional Point-Cloud Data Based on Curvature Map[J]. Journal of Tianjin University(Science and Technology), 2013, 46(2):174-180



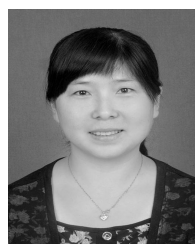
**YANG WEN** is Ph.D. student in the School of Information Science and Technology of Northwest University. His main research interests are image processing, deep learning and pattern recognition.



**GENG GUOHUA** received the Ph.D. degree in computer software and theory from Northwest University, Xi ' an, China, in 2004. Since 2002, she has been a Professor with the School of Information Science and Technology, Northwest University. Her research interests include image processing, intelligent information processing, and the digital restoration of cultural heritage.



**ZHOU MINGQUAN** is a professor at the School of Information Science and Technology of Northwest University, Ph. D. supervisor, and an outstanding member of the Chinese Computer Society. His main research areas are virtual reality, image processing, visualization technology and so on.



**LIU XIAONING** received the Ph.D. degree in computer software and theory from Northwest University, Xi ' an, China, in 2006. Since 2006, she has been an Associate Professor with the School of Information Science and Technology, Northwest University. Her research interests include computer-assisted skull authentication technology, image processing, and machine learning.